A Novel Probabilistic Optimal Power Flow Model with Uncertain Wind Power Generation Described by Customized Gaussian Mixture Model

Deping Ke, C. Y. Chung, *Senior Member*, *IEEE*, and Yuanzhang Sun, *Senior Member*, *IEEE*

Abstract*--A novel probabilistic optimal power flow (P-OPF) model with chance constraints that considers the uncertainties of wind power generation (WPG) and load is proposed in this paper. An affine generation dispatch strategy is adopted to balance the system power uncertainty by several conventional generators, and thus the linear approximation of the cost function with respect to the power uncertainty is proposed to compute the quantile (which is also recognized as the value-at-risk) corresponding to a given probability value. The proposed model applies this quantile as the objective function and minimizes it to meet distinct probabilistic cost regulation purposes via properly selecting the given probability. In particular, the hedging effect due to the used affine generation dispatch is also thoroughly investigated. Besides, an analytical method to calculate probabilistic load flow (PLF) is developed with the probability density function of WPG which is proposed to be approximated by a customized Gaussian mixture model whose parameters are easily obtained. Accordingly, it is successful to analytically compute the chance constraints on the transmission line power and the power outputs of conventional units. Numerical studies of two benchmark systems show the satisfactory accuracy of the PLF method, and the effectiveness of the proposed P-OPF model.

***Index Terms*—Chance constraint, Gaussian mixture model, optimal power flow, probability density function, value-at-risk, wind power generation.**

I. INTRODUCTION

Wind power generation (WPG) has been tremendously developed worldwide so far. This also gives rise to a notable issue that if power systems with highly penetrated WPG still dispatch and operate by conventional deterministic manners, their security and economy can no longer be ensured as confidently as before because of high uncertainties of WPG [1], [2]. Thus, extension of the traditional optimal power flow (OPF) to take into account the uncertainties of WPG has become particularly important and has received increasing attention in recent years [3]-[5].

Actually, the OPF with consideration of load uncertainties has been widely referred to as a probabilistic OPF (P-OPF) problem, and several typical approaches to compute P-OPF include two-point estimation [6], first-order second moment method [7], [8], cumulant method [9], [10], and so on. Their common essence is that the random variables (RVs) which are assumed to be or close to normally distributed are parameterized in the deterministic OPF so that its solutions (cost, node injection, line flow and bus voltage) are implicit functions of these RVs. The first few statistical moments of the solutions are then calculated according to these functions, and thus the probability density functions (PDFs) of the solutions can be approximately constructed. Compared to the methods relying on the implicit relationships between the solutions of the deterministic OPF and the parameterized RVs, it is advocated in [11] that the probabilistic characteristics of all RVs (including the solutions) should be directly incorporated into the optimization problem itself. Therefore, the probability of the event that the total conventional generation plus WPG is not less than the total load being larger than a given value has been used in [11] as a constraint, but the objective function is still deterministic so that the influence of the WPG uncertainties on the total generation cost has not been considered. Similarly, the deterministic objective function is employed in [12] with feasible yet indirect consideration of uncertainties of load flow caused by the WPG. Specifically, a novel and straightforward idea has been utilized to investigate impacts on the generation cost due to the WPG uncertainties by way of penalizing the expected surplus and deficit between the practical WPG and its planed committed value in the objective function of P-OPF model [13]-[15].

Another large category of methods to consider uncertainties in the P-OPF is the chance-constrained OPF (CCOPF) [16]-[21]. A feasible CCOPF model has been proposed in [22] where the expectation of the cost function is minimized, subject to the constraints expressed in terms of occurrence probabilities. However, only uncertainties of loads which are dealt with by the time-consuming Monte Carlo (MC) simulation are considered. Analogous CCOPF model is also constructed in [17] where the back-mapping and the linearization methods simplify the approximate probabilistic calculations during the nonlinear programming. Then, this work is extended by [18] to handle the non-Gaussian distributed WPG involved in the CCOPF model of distribution systems using an analytical approximation method. It is noted that the MC simulation is still required to calculate the derivatives of the chance constraints with respect to the control variables. Particularly, literature [19] considers a chance-constrained unbalance OPF problem with multiple objectives for distribution systems; the efficient two-point estimation is utilized to approximately evaluate the chance constraints. A novel CCOPF method proposed in [20] equivalently transforms the chance constraints into the tractable de-

This work was supported by the National Natural Science Foundation of China (Grant No.: 51307124).

D. P. Ke and Y. Z. Sun are with the School of Electrical Engineering, Wuhan University, Wuhan, China. (e-mail: kedeping@whu.edu.cn; yzsun@mail.tsinghua. edu.cn).

C. Y. Chung is with the Department of Electrical and Computer Engineering, University of Saskatchewan, Saskatoon, Saskatchewan, Canada (c.y.chung@usask.ca).

terministic constraints primarily depending on the hypothesis of Gaussianity of uncertain power sources and loads. Furthermore, literature [21] successfully slacks such Gaussianity assumption on the uncertain power sources; the transformation to the deterministic constraints is also exquisitely fulfilled only requiring the upper and lower bounds of the uncertain power sources' outputs.

One key issue to efficiently integrate the uncertain WPG into P-OPF is to develop a probabilistic model for WPG which has acceptable accuracy and which can also facilitate subsequent probabilistic computing so as to avoid use of MC simulation. The cumulants based expansions, i.e. Gram-Charlier (GC) [23], Edgeworth (EW) [24] and Cornish-Fish (CF) [25] have been used to approximate PDFs of RVs. However, it has been pointed out in [26] that the satisfactory approximation results can be obtained only when the PDFs of RVs are close to normal distribution. Thus, it is generally inaccurate to represent the PDF of WPG directly by these ways because it is naturally far from a normal distribution [27], and large errors may appear around the maximum and minimum power points (tail regions) of the PDF where it is discontinuous [26]. However, [28] attempts to address such weakness through heuristically modifying the result at the discontinuous points when using GC expansion to approximate the PDF of WPG. An innovative Gaussian mixture model (GMM) has been proposed to represent the PDF of WPG so that the probabilistic load flow (PLF) calculation can be analytically accomplished based on the parameters (coefficient, mean and variance) of all Gaussian-Functions (GFs) [29], [30], and the expectation maximization (EM) algorithm is used to recursively generate these parameters. It is inferred that GMM with EM algorithm may need more GFs (e.g., five in [30]) to obtain satisfactory approximation effect for the PDF of WPG because it does not care about the discontinuities of the PDF. So, the computational complexity and time of generating GFs' parameters as well as subsequent PLF would be prominently enhanced as the number of wind farms increases.

Specifically, owing to use of an affine control (dispatch) strategy which recruits conventional generators to proportionally share the duty of balancing the total power (renewable energy sources and loads) uncertainty with respect to its expected value (EV), two pioneer works [20] and [21] deduce the quite favorable analytical characteristics while computing the CCOPF; thus the classic quadratic programming can be utilized to search the optimal solution. In the context of the affine control, the conventional unit's power output consists of two parts: the basic power generation which is decided irrespective of the uncertainty and before the realization of the uncertainty; the adjustable power generation which is proportional to the uncertainty and thus only determined in the meantime with the realization of the uncertainty. The common objective of [20] and [21] is to find the optimal basic power generation and participation factors (proportions) of the conventional units so as to minimize the EV of the total cost. Clearly, the detailed distribution of the cost is not the concern of these researches, which is however the key to reveal the essence of the used affine generation control.

Based on the above review, this paper proposes a novel P-OPF model with chance constraints which delicately copes with uncertainties of WPG and load. Specifically, the affine control is adopted to tackle with the power uncertainty in the proposed model. However, it is proposed to approximately model the cost function as a linear function of the power uncertainty so that its quantile can be readily calculated. Accordingly, the proposed P-OPF model uses a quantile of the cost function corresponding to a given probability value as the objective function. Indeed, this quantile is well recognized as the value-at-risk (VaR) in the field of the risk management. Although the direct interpretation of the VaR minimization is that the cost values in a proportion of stochastic (WPG and load) scenarios indicated by the given probability value are constrained by minimizing the worst-one of them, it also makes clear sense regarding to the optimization of the cost's probability distribution in the context of using the affine control to accommodate the power uncertainty: e.g., according to the given probability value, the high cost occurrence probability can be decreased or the low cost occurrence probability can be increased. What is more, the hedging effect due to the used affine control of the power uncertainty is also thoroughly uncovered. Besides, inspired by the GMM method, the PDF of WPG is proposed to be approximated by a customized GMM which is a linear combination of triple GFs aiming at eliminating impacts of the discontinuities to enhance overall approximation effect. In particular, the parameters of the GFs are readily obtained by the moment matching method. Then, an analytical method is developed for calculating the PLF. Therefore, based on the obtained analytical cumulative probability functions (CDFs) of some RVs, i.e. active power outputs of conventional units and active power flow of transmission lines, the chance constraints on these variables can be readily handled during solving the proposed model.

The remainder of the paper is organized as follows. Section II introduces the affine control to balance the total power uncertainty, and deduces CDFs of the conventional units' power outputs and the cost function. The proposed PLF method based on an approximation of the PDF of WPG is introduced in Section III. Detailed formulations and discussions of the proposed model and the relevant simulation studies are presented in Section IV and V, respectively. Section VI concludes the paper.

II. RVs Raised from Affine Generation Control to Accommodate Power Uncertainty

The proposed P-OPF model uses the quantile of the cost as the objective function and imposes chance constraints on the power outputs of the conventional units which participate in balancing the power uncertainty. So, prior to introduction of the P-OPF model (Section IV), the following two subsections will deduce in detail the CDFs of these RVs which are necessary to evaluate the quantile and chance constraints.

A. CDFs of Power Outputs of Conventional Units Participating in Balancing Uncertainties

Normally, wind power PDFs can be computed from given PDFs of wind speed together with power curves of wind turbines. So, it can be inferred that for a wind turbine, there is a probability mass corresponding to the minimum (zero) power output because of the wind speed smaller than the cut-in value or larger than the cut-off value; and a probability mass corresponding to the maximum (rated) power output due to the wind speed larger than the rated value and smaller than the cut-off value. According to the relationship between the probability density and the probability, the probability mass of the maximum (or minimum) power point should be the integration of this points' probability density over the point. In addition, an impulse function $\delta(x)$ can be simply defined by the following characteristics: i) $\int_{x_0^-}^{x_0^+} A\delta(x-x_0)\,dx=A$ with A denoting the impulse strength; ii) if $x\neq x_0$, then $\delta(x-x_0)=0$. Therefore, it becomes quite obvious that an impulse function can be used to stand for the probability density of the wind turbine's power output at the extreme value point and the impulse strength is the probability mass of this point. Generally, a common shape of wind turbines' power output PDFs is depicted in Fig. 1 [27]. Since generation of all wind turbines in the same wind farm are aggregated into one in this paper, PDF $f_{wi}(\cdot)$ of power output of the ith wind farm can be mathematically described as:

$$f_{wi}\left(p_{wi}\right)=c_{\max i}\delta\left(p_{wi}-p_{\max wi}\right)+c_{\min i}\delta\left(p_{wi}-p_{\min wi}\right)+\theta_i\left(p_{wi}\right) \tag{1}$$

where p_{wi} is the active power output of the ith wind farm; p_{maxwi} and p_{minwi} are the maximum and minimum of p_{wi}; c_{maxi} and c_{mini} represent the strength of the impulses (or probability masses) at p_{maxwi} and p_{minwi}, respectively; and $\theta_i(\cdot)$ is the function depicting the curve between the two impulses. Moreover, following [12], [31], the uncertain loads in this paper are assumed to be normally distributed. Therefore, PDF $f_{Lj}(\cdot)$ of the jth load can be expressed as:

$$f_{Lj}\left(p_{Lj}\right)=g\left(\bar{\mu}_{Lj},\sigma_{Lj},p_{Lj}\right) \tag{2}$$

where p_{Lj} denotes the active power of the jth load; $g(\cdot)$ is the GF; $\bar{\mu}_{Lj}$ and σ_{Lj} are the EV and the standard deviation (STD), respectively. In addition, all RVs are assumed to be mutually independent in this study.

Generally, a RV can be equivalently represented by the sum of its EV (deterministic) and the deviation (uncertain) with respect to the EV. Hence, the alternative forms of (1) and (2) in terms of the deviations are as follows:

$$f_{wi}\left(\Delta p_{wi}\right)=c_{\max i}\delta\left(\Delta p_{wi}-\Delta p_{\max wi}\right)+c_{\min i}\delta\left(\Delta p_{wi}-\Delta p_{\min wi}\right)+\theta_{\Delta i}\left(\Delta p_{wi}\right) \tag{3}$$

$$f_{Lj}\left(\Delta p_{Lj}\right)=g\left(0,\sigma_{Lj},\Delta p_{Lj}\right) \tag{4}$$

with the following auxiliary definitions:

$$\Delta p_{wi}=p_{wi}-\bar{p}_{wi},\ \Delta p_{minwi}=p_{minwi}-\bar{p}_{wi},\ \Delta p_{maxwi}=p_{maxwi}-\bar{p}_{wi},$$
$$\theta_{\Delta i}\left(\Delta p_{wi}\right)=\theta_i\left(\Delta p_{wi}+\bar{p}_{wi}\right),\Delta p_{Lj}=p_{Lj}-\bar{p}_{Lj} \tag{5}$$

where $\bar{p}_{wi}$ and $\bar{p}_{Lj}$ are EVs of p_{wi} and p_{Lj}, respectively; Δp_{wi} and Δp_{Lj} are the deviations of these two RVs from their respective EVs. Consequently, the total uncertain power p_{un} of the system due to the WPG and the uncertain loads is computed as follows:

$$p_{un}=\sum_{j=1}^{N_L}\Delta p_{Lj}-\sum_{i=1}^{N_w}\Delta p_{wi} \tag{6}$$

where N_L and N_w are the numbers of uncertain loads and wind farms, respectively. It can be inferred from (3)-(6) that the EV of p_{un} is zero; p_{un} is positive if the total uncertain load power is larger than the total uncertain wind power, and the overestimation of WPG (with respect to the EV) is simply used to describe this situation. Thus, the underestimation of WPG will mean negative p_{un}. Furthermore, with the given PDFs (3) and (4), CDF of p_{un} denoted by $F_{un}(\cdot)$ can be numerically obtained via MC simulation of (6). Such univariate numerical function is smooth and monotonic and remains unchanged during the optimization. Therefore, when $F_{un}(\cdot)$ is stored in advance as the following series of pairs:

$$\left[p_{un1},F_{un}(p_{un1})\right],\left[p_{un2},F_{un}(p_{un2})\right],\left[p_{un3},F_{un}(p_{un3})\right]\cdots$$

where p_{un1}, p_{un2}, p_{un3},… are uniformly spaced, then its specific evaluation during the optimization can be efficiently fulfilled by the table look-up and the first-order interpolation algorithms.

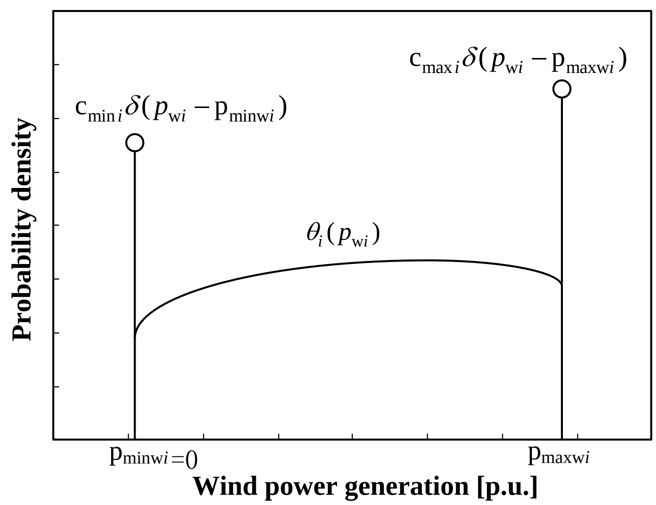

Fig. 1. Common shape of PDF of WPG.

In order to keep balance between active power generation and demand at any given time, p_{un} is usually accommodated by some conventional units. In this paper, a straightforward balancing strategy (affine control) which has been addressed in [20] and [21] is employed to distribute p_{un} among these units proportionally, as follows:

$$p_{tk}=\bar{p}_{tk}+\eta_k p_{un} \qquad \eta_k\geq 0 \qquad k=1,2,...,N_t \tag{7}$$

$$\eta_1+\eta_2+...+\eta_{N_t}=1 \tag{8}$$

where p_{tk} is the active power output of the kth generator which participates in balancing the uncertain power; N_t is the number of this sort of generators; $\bar{p}_{tk}$ is the EV (basic power) of p_{tk}; and η_k is the participation factor. Thus, based on (7), the CDF of p_{tk} denoted by $F_{tk}(\cdot)$ is calculated as:

$$F_{tk}\left(p_{tk}\right)=F_{un}\left(\left(p_{tk}-\bar{p}_{tk}\right)/\eta_k\right) \tag{9}$$

Furthermore, the probability of the event that p_{tk} resides within the allowable range can be obtained as follows:

$$\mathrm{Prob}\left(\mathrm{p}_{\mathrm{min}tk} \le p_{tk} \le \mathrm{p}_{\mathrm{max}tk}\right) = F_{tk}\left(\mathrm{p}_{\mathrm{max}tk}\right) - F_{tk}\left(\mathrm{p}_{\mathrm{min}tk}\right) \quad (10)$$

where $\mathrm{p}_{\mathrm{max}tk}$ and $\mathrm{p}_{\mathrm{min}tk}$ are the upper and lower limits of p_{tk}, respectively.

In practice, the general rules to select the conventional units participating in the accommodation of the uncertain power include: i) the basic requirement is that the selected units should be dispatchable; ii) the selected units should have adequate adjustable capacities; iii) locations of the selected units should not be very electrically far away from uncertain sources. Particularly, use of the third rule just tries to avert the practical transmission congestion (unsolvable AC load flow problem) because the subsequent section will utilize the DC load flow for the PLF analysis so that the transmission congestion cannot be reflected and constrained. Even so, the full AC load flow based validation is still necessarily performed to justify derived solutions.

B. CDF of Cost Function

Following the commonly used quadratic fuel cost function, the total generation cost of the system can be calculated as follows:

$$ct = \sum_{k=1}^{\mathrm{N_t}} \left(\mathrm{a}_k p_{\mathrm{t}k}^2 + \mathrm{b}_k p_{\mathrm{t}k} + \mathrm{c}_k\right) + \sum_{k=\mathrm{N_t}+1}^{\mathrm{N_g}} \left(\mathrm{a}_k p_{\mathrm{t}k}^2 + \mathrm{b}_k p_{\mathrm{t}k} + \mathrm{c}_k\right) \quad (11)$$

where a_k, b_k and c_k are the cost coefficients with the unit of \$/h p.u.; and $\mathrm{N_g}$ denotes the number of conventional units in the system. Specifically, the first summation on the right hand side of (11) denotes the sum of the cost of the generators participating in balancing the uncertain power, while the second summation corresponds to the generators which output deterministic and scheduled power during the practical operation.

By substituting (7) into the first summation on the right hand side of (11) and then rearranging it, the following formulation can be obtained:

$$ct = \varepsilon_0 + \varepsilon_1 p_{\mathrm{un}} + \varepsilon_2 p_{\mathrm{un}}^2 \quad (12)$$

where,

$$\varepsilon_0 = \sum_{k=1}^{\mathrm{N_t}} \left(\mathrm{a}_k \overline{\mathrm{p}}_{\mathrm{t}k}^2 + \mathrm{b}_k \overline{\mathrm{p}}_{\mathrm{t}k} + \mathrm{c}_k\right) + \sum_{k=\mathrm{N_t}+1}^{\mathrm{N_g}} \left(\mathrm{a}_k p_{\mathrm{t}k}^2 + \mathrm{b}_k p_{\mathrm{t}k} + \mathrm{c}_k\right) \quad (13)$$

$$\varepsilon_1 = \sum_{k=1}^{\mathrm{N_t}} \left(2\mathrm{a}_k \overline{\mathrm{p}}_{\mathrm{t}k} \eta_k + \mathrm{b}_k \eta_k\right) \quad (14)$$

$$\varepsilon_2 = \sum_{k=1}^{\mathrm{N_t}} \mathrm{a}_k \eta_k^2 \quad (15)$$

Physically speaking, the cost coefficient a_k in (11) is generally much smaller than b_k [32]-[34]. Moreover, η_k is positive and less than 1.0. Thus, according to (14) and (15), ε_2 is often quite small with respect to ε_1. Furthermore, although p_{un} derived from (6) has an infinite variation range because of the loads with normal distributions, it actually stays within a limited range around zero with a very large probability while rarely appears beyond this range. Consequently, no obvious error is caused if the second-order term of (12) is neglected while calculating the CDF of *ct*. Indeed, this linearization method for probabilistic analysis has been adopted frequently in extant literatures [25], [26]. Hence, the cost function (12) can be approximated as:

$$ct = \varepsilon_0 + \varepsilon_1 p_{\mathrm{un}} \quad (16)$$

Accordingly, the EV of *ct* is approximated by ε_0. As the comparison, the exact calculation of the EV of *ct* is provided in [20] and [21], as follows:

$$\varepsilon_0 + \left(\sum \sigma_{\mathrm{w}i}^2 + \sum \sigma_{\mathrm{L}j}^2\right) \sum_{k=1}^{\mathrm{N_t}} \mathrm{a}_k \eta_k^2 \quad (17)$$

where $\sigma_{\mathrm{w}i}$ is the STD of the *i*th wind farm's power output. The second additive term of (17) is generally much smaller than ε_0 due to the facts presented previously. In addition, it is noted that the uncertainty of *ct* is introduced entirely by the second term on the right hand side of (16) because ε_0 and ε_1 are deterministic. The CDF of *ct* denoted by $F_{\mathrm{ct}}(\cdot)$ can then be obtained by shifting and scaling $F_{\mathrm{un}}(\cdot)$, as follows:

$$F_{\mathrm{ct}}(ct) = F_{\mathrm{un}}\left((ct - \varepsilon_0)/\varepsilon_1\right) \quad (18)$$

Moreover, the quantile corresponding to a probability value *q* can be calculated as follows:

$$ct = F_{\mathrm{ct}}^{-1}(q) = \varepsilon_0 + \varepsilon_1 F_{\mathrm{un}}^{-1}(q) \quad (19)$$

Like the numerical $F_{\mathrm{un}}(\cdot)$ used in the previous subsection, $F_{\mathrm{un}}^{-1}(\cdot)$ can also be numerically stored in advance as the series of pairs but with uniformly spaced probability values. So, given a probability value q, $F_{\mathrm{un}}^{-1}(\mathrm{q})$ can be efficiently evaluated by utilizing the table look-up and the first-order interpolation algorithms, and it will keep fixed during computing the P-OPF.

III. Probabilistic DC Load Flow With Proposed Approximation of PDF of WPG

The chance constraints on the transmission line power are included in the proposed P-OPF model. Thus, before proceeding to this model, this section will derive the CDFs of transmission line power first by the PLF which are based on the DC load flow and proposed approximation of the PDF of WPG.

As mentioned earlier, the cumulants based expansions (GC, EW and CF) often have low accuracy to represent the PDF of WPG because of its discontinuities (two impulses), which can be clearly observed in Fig. 1. Therefore, inspired by the GMM, a novel approximation of $f_{\mathrm{w}i}(\cdot)$ is proposed in this paper, as follows:

$$\begin{aligned} \underline{f}_{\mathrm{w}i}(\Delta p_{\mathrm{w}i}) &= \mathrm{c}_{\mathrm{max}\,i}\,\delta\left(\Delta p_{\mathrm{w}i} - \Delta \mathrm{p}_{\mathrm{max\,w}i}\right) \\ &+ \mathrm{c}_{\mathrm{min}\,i}\,\delta\left(\Delta p_{\mathrm{w}i} - \Delta \mathrm{p}_{\mathrm{min\,w}i}\right) + \mathrm{c}_{\mathrm{w}i}\, g\left(\overline{\mu}_{\mathrm{w}i}, \sigma_{\mathrm{w}i}, \Delta p_{\mathrm{w}i}\right) \end{aligned} \quad (20)$$

with the constraints that the zero, first and second-order moments of $\underline{f}_{\mathrm{w}i}(\cdot)$ should be identical to those of $f_{\mathrm{w}i}(\cdot)$, which can be mathematically described as follows:

$$\mathrm{c}_{\mathrm{max}\,i} + \mathrm{c}_{\mathrm{min}\,i} + \mathrm{c}_{\mathrm{w}i} = 1.0 \quad (21)$$

$$\mathrm{c}_{\mathrm{max}\,i} \Delta \mathrm{p}_{\mathrm{max\,w}i} + \mathrm{c}_{\mathrm{min}\,i} \Delta \mathrm{p}_{\mathrm{min\,w}i} + \mathrm{c}_{\mathrm{w}i} \overline{\mu}_{\mathrm{w}i} = 0 \quad (22)$$

$$\int_{-\infty}^{\infty} x^2 \underline{f}_{\mathrm{w}i}(x)\,dx = \int_{-\infty}^{\infty} x^2 f_{\mathrm{w}i}(x)\,dx \quad (23)$$

Parameters $\mathrm{c}_{\mathrm{w}i}$, $\overline{\mu}_{\mathrm{w}i}$ and $\sigma_{\mathrm{w}i}$ of (20) can be readily calculated from (21)-(23). It is noted that the proposed approximation employs the commonly used moment matching technique to determine its parameters [35]. Besides, it also pays special attention to discontinuities of the exact PDF by directly preserving the two impulse functions. Since the total probabilities at the two discontinuous points is quite significant (no less than 0.4, normally), such particular emphasis is able to greatly enhance the overall approximation effect. Moreover, compared to the impulse strength (probability mass at the discontinuous point), the cumulation of the error between $c_{wi}g(\cdot)$ and $\theta_{\Delta i}(\cdot)$ over a local region around the discontinuous point is generally very limited. Therefore, the proposed approximation is capable of presenting fairly satisfactory approximation effects around the tail region of the CDF. Moreover, due to the fact that an impulse function can be equivalent to a GF with zero STD in the sense of probabilistic computing, the proposed approximation can be regarded as a customized GMM. Here, it should be highlighted that if the customized GMM is compared with the general GMM, the latter is undoubtedly a much more universal and accurate way to model the most non-Gaussian distributions. The primary feature of the customized GMM is its exclusively aiming at the PDF of WPG which however is relatively awkwardly handled by the general GMM. As mentioned and exampled in Section II, the general GMM due to its intrinsic characteristics usually requires more GFs to approximate the PDF of WPG than the customized GMM. Obviously, more GFs mean that more computational burden will be introduced in the subsequent PLF analysis. Moreover, the procedure to obtain the parameters of the general GMM is never as simple as that of the customized GMM.

In the rest of this section, in order to simplify the notations as well as to avoid confusion, the N_w+N_L RVs associated with the WPG and loads are re-denoted by $\Delta p^{(1)}$, $\Delta p^{(2)}$,…, $\Delta p^{(N_w)}$, …, $\Delta p^{(N_w+N_L)}$. Accordingly, $\underline{f}_{wi}(\cdot)$ and $f_{Lj}(\cdot)$ are replaced by $f^{(i)}(\cdot)$ and $f^{(j)}(\cdot)$, respectively. So, the PDF of the ith WPG can be approximated based on (20), as follows:

$$f^{(i)}\left(\Delta p^{(i)}\right)=\sum_{k=1}^{3}\mathrm{c}_k^{(i)}g\left(\bar{\mu}_k^{(i)},\sigma_k^{(i)},\Delta p^{(i)}\right) \tag{24}$$

where,

$$\begin{aligned}
&\mathrm{c}_1^{(i)}=\mathrm{c}_{\max i}, \quad \bar{\mu}_1^{(i)}=-\Delta \mathrm{p}_{\max i}, \quad \sigma_1^{(i)}=0;\\
&\mathrm{c}_2^{(i)}=\mathrm{c}_{\min i}, \quad \bar{\mu}_2^{(i)}=-\Delta \mathrm{p}_{\min i}, \quad \sigma_2^{(i)}=0;\\
&\mathrm{c}_3^{(i)}=\mathrm{c}_{wi}, \quad \bar{\mu}_3^{(i)}=\bar{\mu}_{wi}, \quad \sigma_3^{(i)}=\sigma_{wi}
\end{aligned} \tag{25}$$

Meanwhile, the jth load PDF can be described as:

$$f^{(j)}\left(\Delta p^{(j)}\right)=g\left(0,\sigma_{\mathrm{L}}^{(j)},\Delta p^{(j)}\right) \tag{26}$$

So far, it can be observed from (24) that the PDF of WPG has been actually approximated by a linear combination of triple GFs.

Besides the already quite attractive accuracy, the ultimate merit of the proposed approximation lies in its compatibility to the analytical PLF analysis. Since DC load flow, which can easily establish the linear mappings from node injections to line flow, has been widely adopted to study the stochastic characteristics of line flow under the influences of uncertain node injections [12], [23], it is continuously employed in this paper. Consequently, as EVs of WPG and loads are known, EV of the power flow carried by line s-t denoted by $\bar{\mathrm{p}}^{(s\text{-}t)}$ can be directly solved from the DC load flow. Moreover, with further consideration of (7), the linear relationship between the power flow deviation of the line s-t and the RVs associated with WPG and loads can be obtained as follows:

$$\Delta p^{(s\text{-}t)}=\beta_{st}^{(1)}\Delta p^{(1)}+\beta_{st}^{(2)}\Delta p^{(2)}+\cdots+\beta_{st}^{(N_w+N_L)}\Delta p^{(N_w+N_L)} \tag{27}$$

where $\beta_{st}^{(1)},\beta_{st}^{(2)},...,\beta_{st}^{(N_w+N_L)}$ are the constant coefficients.

Before proceeding to PLF analysis based on (24)-(27), it is necessary to introduce three properties of probabilistic computing [35]: x_1 and x_2 are two independent RVs and their PDFs are $f^{(x_1)}(\cdot)$ and $f^{(x_2)}(\cdot)$, respectively. x_3 is a linear function of them and its PDF is $f^{(x_3)}(\cdot)$. Therefore,

- if x_3=h_1x_1 where h_1 is a constant, then $f^{(x_3)}(x_3)$= $f^{(x_1)}(x_3/h_1)/h_1$;
- if x_3=x_1+x_2, then $f^{(x_3)}(x_3)$=$f^{(x_1)}(x_3)\otimes f^{(x_2)}(x_3)$ where $\otimes$ is the convolution operator;
- if x_1 and x_2 are normally distributed and x_3=x_1+x_2, then x_3 is still normally distributed with the EV equal to the sum of EVs of x_1 and x_2, and the variance (squared STD) equal to the sum of variances of x_1 and x_2.

Hence, according to the properties shown above, PDF of the line power $p^{(s\text{-}t)}$ can be analytically derived based on (24)-(27), as follows:

$$f^{(s\text{-}t)}\left(p^{(s\text{-}t)}\right)=\sum_{k=1}^{3}\sum_{m=1}^{3}\cdots\sum_{n=1}^{3}\mathrm{c}^{(s\text{-}t)}g\left(\bar{\mu}^{(s\text{-}t)},\sigma^{(s\text{-}t)},p^{(s\text{-}t)}\right) \tag{28}$$

where $\mathrm{c}^{(s\text{-}t)}$, $\bar{\mu}^{(s\text{-}t)}$ and $\sigma^{(s\text{-}t)}$ are the symbolic replacements of the following expressions:

$$\mathrm{c}^{(s\text{-}t)}=\mathrm{c}_k^{(1)}\mathrm{c}_m^{(2)}\cdots\mathrm{c}_n^{(N_w)} \tag{29}$$

$$\bar{\mu}^{(s\text{-}t)}=\bar{\mathrm{p}}^{s\text{-}t}+\beta_{st}^{(1)}\bar{\mu}_k^{(1)}+\beta_{st}^{(2)}\bar{\mu}_m^{(2)}+...+\beta_{st}^{(N_w)}\bar{\mu}_n^{(N_w)} \tag{30}$$

$$\begin{aligned}
\left(\sigma^{(s\text{-}t)}\right)^2=&\left(\beta_{st}^{(1)}\sigma_k^{(1)}\right)^2+\left(\beta_{st}^{(2)}\sigma_m^{(2)}\right)^2+\cdots+\left(\beta_{st}^{(N_w)}\sigma_n^{(N_w)}\right)^2\\
&+\left(\beta_{st}^{(N_w+1)}\sigma_{\mathrm{L}}^{(N_w+1)}\right)^2+...+\left(\beta_{st}^{(N_w+N_L)}\sigma_{\mathrm{L}}^{(N_w+N_L)}\right)^2
\end{aligned} \tag{31}$$

The corresponding CDF of $p^{(s\text{-}t)}$ is deduced as follows:

$$\begin{aligned}
F^{(s\text{-}t)}\left(p^{(s\text{-}t)}\right)&=\int_{-\infty}^{p^{(s\text{-}t)}}f^{(s\text{-}t)}\left(x\right)dx\\
&=\sum_{k=1}^{3}\sum_{m=1}^{3}\cdots\sum_{n=1}^{3}\mathrm{c}^{(s\text{-}t)}\int_{-\infty}^{p^{(s\text{-}t)}}g\left(\bar{\mu}^{(s\text{-}t)},\sigma^{(s\text{-}t)},x\right)dx\\
&=\sum_{k=1}^{3}\sum_{m=1}^{3}\cdots\sum_{n=1}^{3}\mathrm{c}^{(s\text{-}t)}\int_{-\infty}^{\frac{p^{(s\text{-}t)}-\bar{\mu}^{(s\text{-}t)}}{\sigma^{(s\text{-}t)}}}g\left(0,1,x\right)dx\\
&=\sum_{k=1}^{3}\sum_{m=1}^{3}\cdots\sum_{n=1}^{3}\mathrm{c}^{(s\text{-}t)}G\left(\frac{p^{(s\text{-}t)}-\bar{\mu}^{(s\text{-}t)}}{\sigma^{(s\text{-}t)}}\right)
\end{aligned} \tag{32}$$

where $G(\cdot)$ denotes the CDF of the standard GF. The accuracy of (32) can be examined via comparison with the CDF derived from the MC simulation. More specifically, the MC simulation first uses the simple random sampling technique to generate WPG samplings (i.e., each sampling denotes the concurrent power outputs of the wind farms) based on the exact PDFs of WPG (Fig. 1). Then, the full AC load flow (without any linearization) is calculated with each WPG sampling and the exact value of $p^{(s\text{-}t)}$ is obtained. Finally, cumulating all these values after the AC load flow calculations synthesizes the CDF of $p^{(s\text{-}t)}$. As the MC simulation normally employs a fairly large number of samplings to adequately capture the stochastic nature of the RVs (in this study the number of the samplings is set to be 20000) and no approximation is used during the load flow computation, the above derived CDF shall be highly accurate so that it can be used as the benchmark for the validation of (32). Thus, the examples of comparing (32) and the CDF obtained by the MC simulation will be presented in Section V.

The probability that $p^{(s\text{-}t)}$ will not exceed the carried power limit $\mathrm{p}_{\max}^{(s\text{-}t)}$ of line *s-t* can be computed as follows:

$$\mathrm{Prob}\left(\left|p^{(s\text{-}t)}\right| \le \mathrm{p}_{\max}^{(s\text{-}t)}\right) = F^{(s\text{-}t)}\left(\mathrm{p}_{\max}^{(s\text{-}t)}\right) - F^{(s\text{-}t)}\left(-\mathrm{p}_{\max}^{(s\text{-}t)}\right) \quad (33)$$

IV. Proposed P-OPF Model

A. Formulation

On the basis of preliminary knowledge presented in Section II and III, the proposed P-OPF model is formulated as follows:

$$\min_{\mathbf{x}_{\mathrm{p}}} \ \mathrm{ct} = F_{\mathrm{ct}}^{-1}(\mathrm{q}) = \varepsilon_0 + \varepsilon_1 F_{\mathrm{un}}^{-1}(\mathrm{q}) \quad (34)$$

$$\text{s.t.} \quad \mathrm{p}_{\mathrm{min}tk} \le p_{tk} \le \mathrm{p}_{\mathrm{max}tk} \qquad k = \mathrm{N_t}+1, \ldots, \mathrm{N_t}+\mathrm{N_g} \quad (35)$$

$$\mathrm{Prob}\left(\left|p^{(s\text{-}t)}\right| \le \mathrm{p}_{\max}^{(s\text{-}t)}\right) \ge \mathrm{q}^{(s\text{-}t)} \quad \text{all } s\text{-}t \in \{\text{branches}\} \quad (36)$$

$$\mathrm{Prob}\left(\mathrm{p}_{\mathrm{min}tk} \le p_{tk} \le \mathrm{p}_{\mathrm{max}tk}\right) \ge \mathrm{q}^{tk} \qquad k = 1, 2, \ldots, \mathrm{N_t} \quad (37)$$

where q, $\mathrm{q}^{(s\text{-}t)}$ and q^{tk} are the given probability values; ct is the quantile corresponding to q; and $\mathbf{x}_{\mathrm{p}}$ is the tunable vector of parameters consisting of EVs ($\bar{\mathrm{p}}_{tk}$) and participation factors (η_k) associated with the conventional units taking part in balancing the power uncertainties, and the power outputs (p_{tk}) of the rest of conventional units. So, (35) is the boundary constraints on the deterministic power outputs of those units.

B. Chance Constraints

Individual chance constraints (36) and (37) are imposed on the power carried by transmission lines and the power output by the conventional units which accommodate the system power imbalance, respectively. However, it should be emphasized that from a more critical perspective, constraining the power of these devices ought to employ the joint probability as follows:

$$\mathrm{Prob}\begin{pmatrix} \left|p^{(s\text{-}t)}\right| \le \mathrm{p}_{\max}^{(s\text{-}t)}, \quad \mathrm{p}_{\mathrm{min}tk} \le p_{tk} \le \mathrm{p}_{\mathrm{max}tk}, \\ \text{all } s\text{-}t \in \{\text{branches}\} \text{ and } k = 1, 2, \ldots, \mathrm{N_t} \end{pmatrix} \quad (38)$$

Here, (38) denotes the probability of these devices' power simultaneously lying within their physical limits. For instance, the probability of simultaneous contingencies is restricted in [36] for the wind integrated unit commitment problem. The scenario approach is employed to make the problem analytically solvable though the computational complexity is remarkable when the number of simultaneous contingencies is large. In fact, exact evaluation of (38) is quite numerically cumbersome as the joint distribution of the RVs involved is required [37]. Particularly, by assuming linear relationship and normal distribution, literature [38] equivalently replaces the joint chance constraints by a set of individual chance constraints when dealing with the long-term voltage control problem. Normally, for the sake of computational simplicity, the joint chance constraint can be approximated by the individual chance constraints although the derived results based on the latter tend to be optimistic [18], [37]. A comprehensive comparisons of these two chance constraint problems are presented in [39] by taking the reservoir management issue as the example.

The parameters $\mathrm{q}^{(s\text{-}t)}$ and q^{tk} could be selected to be close to 1.0 so as to lower the distinction between the joint chance constraint and the individual chance constraints. This actually permits the occurrence possibility of some rare events in which the constraints may be violated; the overall operational economy would be remarkably deteriorated if the constraints in these events are strictly satisfied. Moreover, mathematically speaking, these two parameters cannot reach 1.0 since the RVs derived by the probabilistic calculations with GFs in the previous section extend to both positive and negative infinity.

C. Impacts of Probability q on Optimization Solutions

It is already known that the CDF of *ct* can be approximately obtained by shifting (ε_0) and scaling (ε_1) the CDF of p_{un} which is fixed. Hence, the CDF of *ct* can be only altered (optimized) on its position (by shifting) and profile (by scaling). Specifically, the EV of *ct* (17) is commonly employed by [20] and [21] as the objective to be optimized. This is almost equivalent to minimizing the rightward movement (ε_0) of the CDF of *ct* because ε_0 is always much larger than the second additive term of (17). However, in doing so the CDF's profile is not the concern of the optimization. Therefore, this paper proposes to minimize a more flexible objective function (34) which is the weighted sum of ε_0 and ε_1 ($F_{\mathrm{un}}^{-1}(\mathrm{q})$ plays the role of the weight). In other words, the CDF of *ct* is optimized simultaneously on the shifting and scaling of the CDF of p_{un}. Obviously, the probability q controls the final optimization effects through the weight $F_{\mathrm{un}}^{-1}(\mathrm{q})$: e.g., if q is chosen to be far away from a specific value q_0 which leads to $F_{\mathrm{un}}^{-1}(\mathrm{q}_0)=0$, the distribution of the uncertain part of the generation cost will also be remarkably optimized. So, compared to the exclusive minimization of ε_0, additionally including the uncertainty of the cost in the optimization could be at the expense of increasing the expected cost.

Indeed, selecting q can be profoundly interpreted in terms of the risk management because (34) is a typical VaR minimization problem. Actually, the methodologies associated with VaR and/or conditional VaR have been intensively studied by power system academia. In particular, the power market researches give considerable attentions to the VaR, conditional VaR and their optimization [40]-[42]. Moreover, the applications are also involved in many other aspects of power engineering such as economic operation and dispatch [43], [44], reliability assessment [45], security assessment [46]-[47] and so on. In [44], the conditional VaR is used to construct a regularizer for the convex programming to obtain an intelligent risk-aware dispatch which mitigates the high risk of inadequate wind power in a wind-integrated power system. Literature [45] develops a systematic procedure to implement the VaR based reliability assessment for distribution systems. Specifically, investigating cyber security of smart grids in [46] estimates the defender's loss by a conditional VaR index which is equivalently derived as the load shed in the scenario simulations; a stochastic security game model is solved to find the protective countermeasure which optimizes the VaR index. Moreover, the VaR and conditional VaR based blackout risk indexes have been proposed in

[47] to indicate critical characteristics of blackouts and evaluate security level of power systems. Here, in the proposed O-OPF model the VaR based objective function also presents obvious significance regarding the probabilistic cost management which will be addressed in detail in the following.

Expression (16) indicates that the total generation cost (*ct*) is (approximately) equal to the expected cost (ε_0) plus the uncertainty of extra expense/saving ($\varepsilon_1 p_{un}$) which is produced by the overestimation (p_{un}>0)/underestimation (p_{un}<0) of WPG. Firstly, if q>q_0, the extra expense will fall within the interval [0, $\varepsilon_1 F_{un}^{-1}$(q)] with the confidence level of q-q_0; the proposed optimization obviously makes sense to compress this interval by reducing ε_1. Furthermore, according to the previous shifting and scaling explanation, a smaller ε_1 leads to a smaller cumulative probability of the total cost from a specific large value to the positive infinity (briefly, the occurrence probability of the high cost is reduced). In contrast, the optimization will expand the interval [$\varepsilon_1 F_{un}^{-1}$(q), 0] where the extra saving locates with the confidence level of q_0-q by increasing ε_1 when q<q_0; the cumulative probability of the total cost from the negative infinity to a specific small value becomes larger as ε_1 is larger (briefly, the occurrence probability of the low cost will be magnified). Therefore, it is readily seen that the extra expense/saving sides of the cost uncertainty's CDF cannot be simultaneously optimized because they pose opposite requirements on the scaling factor ε_1. In other words, given any q, the (hedged) solution can only benefit one (either the expense or saving) side but deteriorate another side, e.g. favorably decrease the high cost's occurrence probability but unfavorably decrease the low cost's occurrence probability. Specifically, if |q-q_0| gets larger (q is farther away from q_0), it becomes more confident that the extra expense (saving) is within the corresponding interval while the optimization also gives more priority to compress (expand) the interval with respect to decreasing ε_0. However, on the contrary, the extra saving (expense) side of the cost uncertainty's CDF will be more adversely altered as well. Indeed, this contradictive phenomenon is due to the employed proportional balancing strategy of the uncertain power (it is definitely possible to optimize the overall distribution of the cost uncertainty if a more complex balancing strategy is utilized).

Like the traditional OPF model, the proposed P-OPF model can be handled as a typical constrained nonlinear programming problem where the objective function and the constraints are smooth and differentiable with respect to the tunable parameters. Thus, the efficient sequential quadratic programming (SQP) method developed for this sort of optimizations is adopted in this paper to solve (34)-(37) [48]. The embedded function *fmincon* in the MATLAB Toolbox is utilized to implement this algorithm. Furthermore, this study uses different feasible initial solutions (means all constraints are satisfied) to run the SQP, respectively, so as to enhance the solution's quality; the best final solution which results in the minimum objective function among these runs is adopted.

V. Example Studies

A. IEEE Reliability Test System

The proposed P-OPF model is first implemented in a modified 24-bus IEEE reliability test system where three wind farms are connected to Bus 4, 16 and 17 (the conventional unit originally connected to Bus 16 is discarded), respectively. The diagram and data this system can be found in [49]. The three PDFs of the WPG are assumed to be identical and are derived based on PDF of wind speed and the power curve of wind turbine given in Appendix (Data A). Particularly, the active power loads of Bus 4, 16 and 17 are additionally increased by the EVs of the three wind farms' WPG, respectively. The ratio $\sigma_{Lj}/\bar{\mu}_{Lj}$ is uniformly set to be 7% for the stochastic loads. In addition, active power loads with EVs larger than 180MW are stochastically modeled while the remaining loads use the deterministic models. Thus, there are 3 RVs for the WPG and 10 RVs for the loads in the P-OPF model. Specifically, the penetration level of WPG is about 23% when the EVs of these RVs are employed for the calculation. Table I shows the used cost coefficients and power limits of the conventional units. Thus, except G_{15} and G_{21} which have rather limited adjustable ranges of the active power outputs, it is supposed that G_1, G_2, G_7, G_{13}, G_{18}, G_{22} and G_{23} are employed to balance the uncertain power. In this study, all $q^{(s\text{-}t)}$ and q^{tk} are uniformly set to be 97%.

TABLE I
Data of Conventional Units

	$P_{\mathrm{min}tk}$	$P_{\mathrm{max}tk}$	a_k	b_k	c_k
G_1	0.80	5.60	55.0	1476.0	267.0
G_2	0.90	8.30	40.3	915.0	383.0
G_7	1.00	7.80	42.5	966.3	328.3
G_{18}	1.30	8.60	38.0	900.0	270.0
G_{22}	0.60	7.50	30.7	895.0	220.0
G_{13}	1.50	7.50	8.40	528.5	128.0
G_{15}	1.50	4.20	6.00	550.0	162.0
G_{21}	1.00	4.80	5.50	570.0	143.0
G_{23}	1.20	7.20	7.50	513.7	111.0

TABLE II
Optimal Solution (q=0.5194)

	η_k	$\Sigma\eta_k$	$\bar{p}_{tk}$	$\Sigma\bar{p}_{tk}$
G_1	0.0081	0.5292	0.8692	9.2720
G_2	0.0963		1.7294	
G_7	0.1475		2.2803	
G_{18}	0.0778		2.0644	
G_{22}	0.1995		2.3287	
G_{13}	0.2218	0.4708	5.4038	19.2280
G_{15}	-		4.1842	
G_{21}	-		4.8056	
G_{23}	0.2490		4.8344	

In order to minimize the EV of the cost, q is set to be 0.5194 so that F_{un}^{-1}(q)=0. Then, four search runs by the SQP with different feasible initial solutions are conducted, and the evolutions of the objective function during the search are depicted in Fig. 2. It is seen that these search runs finally converge to the same optimal point (presented in Table II) and are terminated due to the first-order optimality measure less than the specified value. In addition, the search runs averagely take about 8 iterations (cost the computational time of about 3.73s on a PC with Intel Core i5-2320 CPU@3.00GHz and 4G RAM) to converge.

For the subsequent comparisons, Table III and IV also list the optimal solutions obtained by the SQP when q is set to be 0.99 and 0.23, respectively.

TABLE III
OPTIMAL SOLUTION (q=0.99)

	η_k	$\Sigma\eta_k$	$\bar{p}_{tk}$	$\Sigma\bar{p}_{tk}$
G_1	0.0001	0.3517	0.9162	11.2047
G_2	0.0193		2.4982	
G_7	0.0048		3.1111	
G_{18}	0.1296		2.3913	
G_{22}	0.1980		2.2878	
G_{13}	0.3240	0.6483	4.4084	17.2953
G_{15}	-		4.0465	
G_{21}	-		4.7340	
G_{23}	0.3243		4.1064	

TABLE IV
OPTIMAL SOLUTION (q=0.23)

	η_k	$\Sigma\eta_k$	$\bar{p}_{tk}$	$\Sigma\bar{p}_{tk}$
G_1	0.0121	0.8090	0.9045	11.6443
G_2	0.1504		2.2846	
G_7	0.0985		1.8622	
G_{18}	0.2742		3.6547	
G_{22}	0.2737		2.9383	
G_{13}	0.1910	0.1910	4.6804	17.8557
G_{15}	-		3.3345	
G_{21}	-		4.4964	
G_{23}	0.0000		5.3443	

Naturally, the obtained result can be deemed authentic only when the approximation techniques used in the proposed model can have satisfactory accuracy. Therefore, the proposed customized GMM, GC, EW and CF expansions are compared in terms of CDF of the WPG in Fig. 3. Specifically, the first 10 terms are used in the GC expansion, and the first 5 cumulants are contained in expansions of EW in power of $n^{-3/2}$ and CF (if more terms are included in the three expansions, their accuracies are not obviously improved but the computational complexities are greatly increased). It is observed that the proposed method presents fairly acceptable overall approximation effect and also remarkably outperforms the other three methods (especially around the step-change points). As mentioned in the beginning of Section III, such phenomenon is attributed to the fact that the discontinuities in the PDF of WPG are successfully handled by the proposed method. Subsequently, as the solution in Table II is employed, the CDFs of transmission lines' power are derived by the DC load flow based PLF with the approximated PDF of WPG; they are compared with the CDFs derived by the MC simulation introduced in Section III. It is found that the approximated CDFs of all the transmission lines which are obtained by (32) can accurately capture the stochastic properties of the line flows. As an example, Fig. 4 illustrates the CDF of the active power flow carried by the line #2-6. This indeed further validates the effectiveness of the proposed customized GMM to approximate the PDF of WPG and its applications in the PLF analysis. Finally, the linear approximation of the cost is examined (with the solution in Table II) by directly comparing the function curves of (12) and (16) (left plot of Fig. 5). Furthermore, numerical CDFs of the cost computed based on (12) and (16) respectively are also compared in the right plot of Fig. 5. Thus, it is easily noted that the linear approximation has quite satisfactory accuracy over a large range of p_{un} ([-20, 20]). Because p_{un} has little probability to stands far beyond this range, the CDF derived based on the linear approximation can accurately tracks the exact CDF (the solid and dash lines in the right plot of Fig. 5 are almost overlapped).

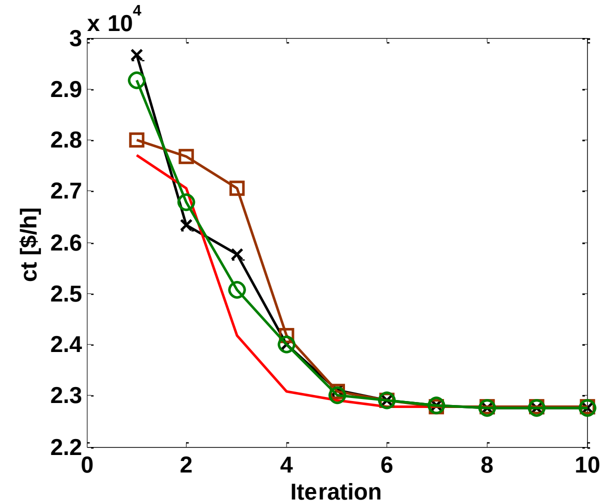

Fig. 2. Four search runs by the SQP with different feasible initial solutions.

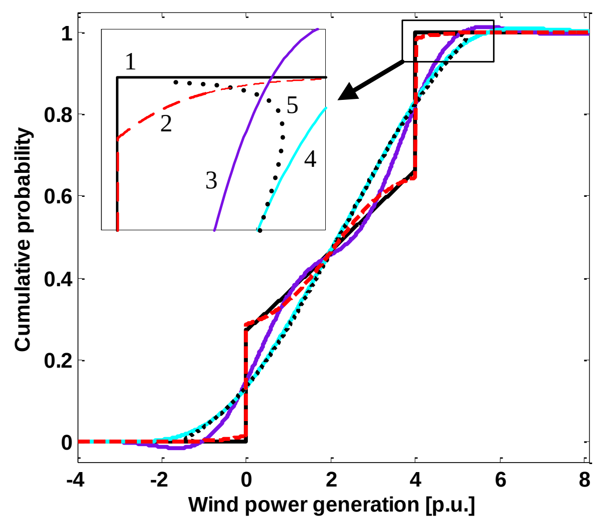

Fig. 3. CDFs of WPG (1-exact; 2-proposed; 3-GC; 4-EW; 5-CF).

Based on the solutions presented in Table II, III and IV, the CDFs of *ct* are calculated and shown in Fig. 6. Moreover, the CDFs are also demonstrated in a decomposed manner by the EV (ε_0) and the CDF of the cost uncertainty (Fig. 7). From these figures, it is easily seen that among the three cases, the CDF of *ct* derived based on the solution in the case of q=0.99 has the most favorable high cost section (larger than 2.6×10^4) while its low cost section (lower than 2.1×10^4) is the worst. Interestingly, the situation is entirely reverse in the case of q=0.23. Indeed, such hedging phenomenon of the solutions is further observed by the statistical data given in Table V. Obviously, the operations of compression and expansion on the CDF of the cost uncertainty in the case of q=0.5194 which are clearly depicted in Fig. 7 graphically account for this phenomenon. Besides, the data provided in Table II, III and IV can also help to uncover the essence of the employed affine generation control which tends to obtain a hedged solution, in the following paragraph.

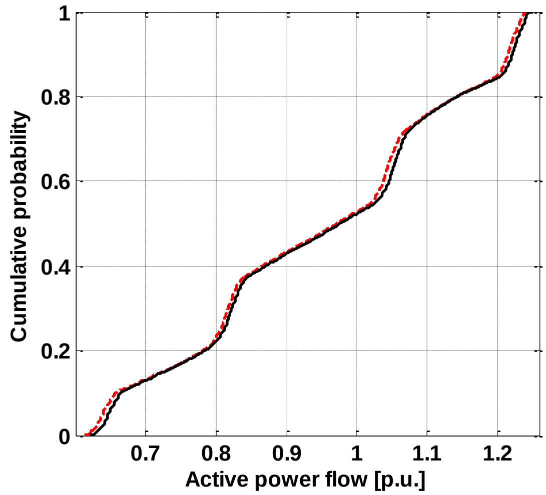

Fig. 4. CDF of active power flow carried by transmission line #2-6 (solid line-proposed method; dash line-MC simulation).

Depending on the cost coefficients of the conventional units presented in Table I, they can be simply and roughly classified into two groups: expensive units (G_1, G_2, G_7, G_{18} and G_{22}) and cheap units (G_{13}, G_{15}, G_{21} and G_{23}). In the case of q=0.5194 where the cost uncertainty is not considered, the cheap units generally tend to output the basic power ($\overline{\mathrm{p}}_{tk}$) as much as possible while the expensive units supply the rest basic (expected) loads so that the EV (ε_0) of *ct* could be minimal. Therefore, the cheap units provide the contribution to balance the power uncertainty as less as possible due to their upper bounds on the power outputs, and the remainder is just accommodated by the expensive units. Then, if overestimation of the WPG really happens (p_{un}>0), the expensive units will take the most duty to balance the uncertain power, leading to the high extra expense. In contrast, this high extra expense risk is considered in the case of q=0.99 and the cheap units less their basic power outputs and reserve more capacities so as to take more duty to balance the power uncertainty (these can be checked from Table II and III by comparing the total basic power outputs $\Sigma\overline{\mathrm{p}}_{tk}$ of the cheap and the expensive units, and the sum $\Sigma\eta_k$ of their participation factors, respectively) so that the extra expense is obviously decreased. Then, the actual cost equal to the EV plus the extra expense will be effectively reduced although the EV is somewhat increased by the more power outputs of the expensive units. On the contrary, compared to the solution in Table II, the solution in Table III would be rather unfavorable if the underestimation of WPG (p_{un}<0) occurs since the increased EV together with less extra saving (here, extra saving is denoted by its absolute value for the sake of expression simplicity though it is essentially negative) results in a larger cost value. So, the optimization with q=0.23 considers the low extra saving risk and enforces the expensive units to play more significant roles in balancing the power uncertainty so that the extra saving is increased (see $\Sigma\eta_k$ in Table II and IV). Furthermore, in order to enlarge the participation factors of the expensive units, their basic power outputs should be increased so that the necessary downward adjustable capacities are available (see $\Sigma\overline{\mathrm{p}}_{tk}$ in Table II and IV). However, although outputting more basic power by the expensive units will increase the EV, the cost is still comparatively reduced due to the increased extra saving. So far, it is not difficult to understand that the solution in Table IV will be much less exhilarated if the overestimation of WPG happens.

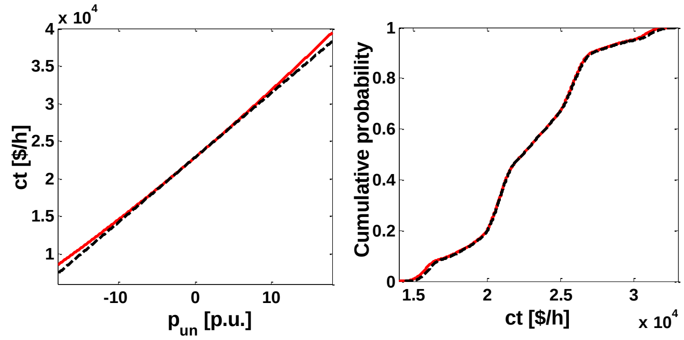

Fig. 5. Function curve and CDF of cost (solid line-exact; dash line-approximate)

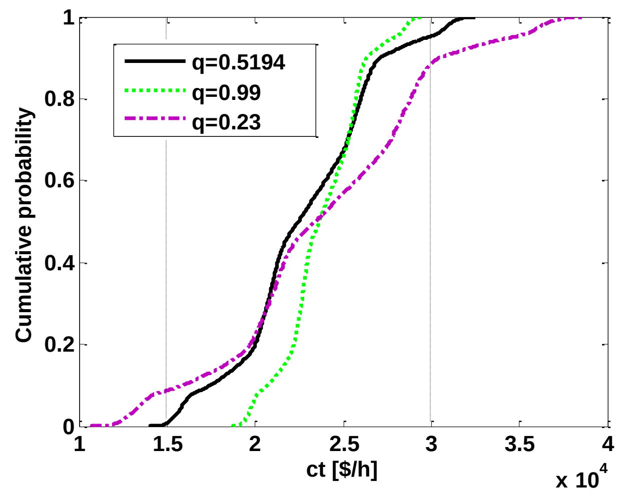

Fig. 6. Optimized CDFs of cost by selecting different values of q.

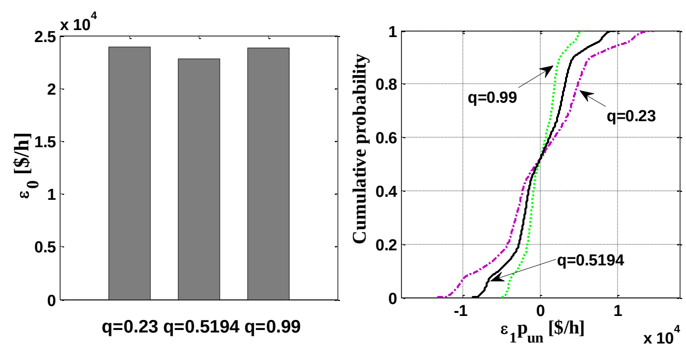

Fig. 7. ε_0 and CDF of cost uncertainty.

Particularly, no matter which (high cost or low cost) section of the CDF of *ct* is ameliorated, it is noted that the EV of *ct* is always sacrificed with respect to the result in the case of q=0.5194. It is already known that as q is selected to be farther away from q_0, this sacrifice will possibly become more serious, which could considerably counteract the improvement of the extra expense/saving. In fact, in this simulated system if q is set to be less than 0.17, the benefit of enhancing the extra saving will be entirely overridden by the adverse impact of increasing the EV.

Although the above simulations are conducted at the same load level, it is seen that the contributions of the units to the uncertain power balance vary remarkably according to the probabilistic cost regulation purposes. For example, G_{23} is a primary unit to accommodate the power uncertainty in the case of q=0.99 while it is totally free from this task and only outputs the basic power in the case of q=0.23. Moreover, no chance constraint on the transmission line power is activated and the constraints on the conventional units' power outputs have the most impact on the final solutions in the three cases. For example, the solution in Table IV activates the lower bounds of the chance constraints on the power outputs of G_{18} and G_{22}. Indeed, the transmission line power constraints can also considerably influence η_k and $\bar{p}_{tk}$ of the conventional units. So, a new simulation case with the EVs of the loads at Bus 3, 5, 9, and 10 increased by 20% is conducted. As q=0.99 is employed again, the solution of the optimization is given in Table VI. It is found that the solution activates the upper bounds of the chance constraints on the power of transmission lines #15-24, #20-12 and #13-11 which are the important corridors to deliver power from G_{15}-G_{23} to the load center. Therefore, compared to the situation in Table III, G_1, G_2 and G_7 output more basic power and take more duty to balance the power uncertainty. Moreover, it is also seen that the power output of G_1 is almost deterministic (η_k is fairly small) in the low load level case (Table III) but it is recruited to share the balancing duty with other units as the load level is increased (Table VI).

TABLE V
OCCURRENCE PROBABILITIES OF LOW COST AND HIGH COST

	q=0.23	q=0.5194	q=0.99
Prob(ct<1.5×10^4)	0.0875	0.0074	0
Prob(ct>3.0×10^4)	0.1107	0.0463	0

TABLE VI
OPTIMAL SOLUTION WITH INCREASED LOAD LEVEL (q=0.99)

	η_k	$\Sigma\eta_k$	$\bar{p}_{tk}$	$\Sigma\bar{p}_{tk}$
G_1	0.1223	0.4895	2.0402	14.1508
G_2	0.0993		3.5321	
G_7	0.1348		4.1235	
G_{18}	0.0636		2.1020	
G_{22}	0.0695		2.3530	
G_{13}	0.2270	0.5105	5.2082	19.5067
G_{15}	-		4.9435	
G_{21}	-		5.1120	
G_{23}	0.2835		4.2430	

B. IEEE 118-Bus System

In this subsection, robustness of the proposed model with respect to a different system is tested. Thus, the modified IEEE 118-bus system where five wind farms are used to replace the conventional generators at Bus 15, 42, 90, 99 and 116 is employed. The five CDFs of the WPG are also assumed to be identical, and the data (Data B) in Appendix is used to compute them. Moreover, there are a total of 11 RVs relevant to the active power loads with EVs larger than 75MW, and $\sigma_{Lj}/\bar{\mu}_{Lj}$ is uniformly set to be 5%. Thus, the penetration level of WPG is about 19%. Furthermore, the conventional units at Bus 12, 19, 31, 34, 46, 54, 61, 74, 77 and 111 which have adequate adjustable capacities and are electrically adjacent to the wind farms are employed to balance the uncertain power. All $q^{(s\text{-}t)}$ and q^{tk} are set to be 97%. The other details and data of this system can be found in [50]. Due to the increased number of decision variables (totally 59) and wind farms, the computational scale of the P-OPF for this system is much larger than that for the previous simulated system. However, the P-OPF herein is still efficiently solved by the SQP; it takes about 15.40s on average to converge (with the same computational platform used in the previous subsection) as q is selected to be different values.

Definitely, the solution of the P-OPF makes sense only when the employed approximations are acceptably accurate. Thus, based on the solution in the case of q=0.99, the left plot of Fig. 8 shows the CDF of the linearly approximate cost which satisfactorily tracks the exact CDF. Moreover, it is also found that all the transmission lines have the approximate CDFs of the power which are with acceptable accuracy, and an example is provided in the right plot of Fig. 8. All these simulation results are the strong evidence to again support the feasibility of the proposed linearization of the cost function to obtain CDF and the effectiveness of approximating the PDF of WPG by a customized GMM.

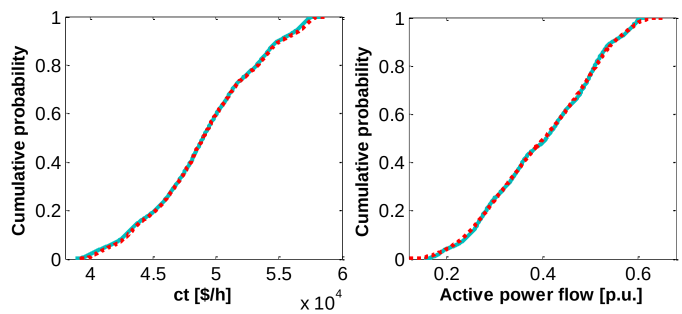

Fig. 8. CDFs of cost and active power flow carried by line #69-47 (solid line-exact; dash line-approximate).

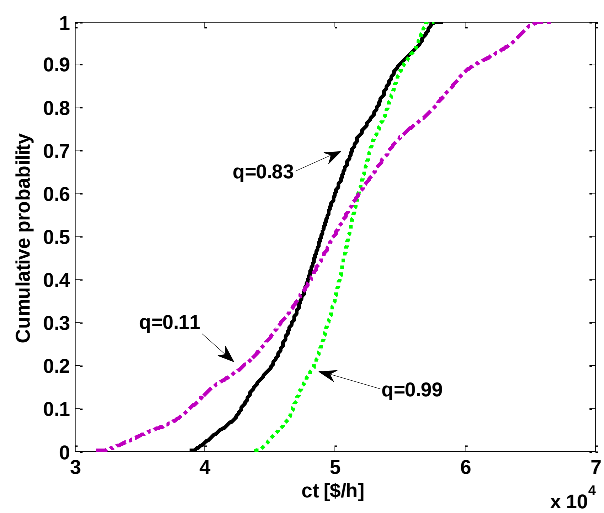

Fig. 9. Optimized CDFs of cost by selecting different values of q.

As conducted in the previous study, the solutions are obtained when q is selected to be 0.11, 0.83 and 0.99, respectively; they are compared in terms of the CDF of *ct* (Fig. 9). The intention in the case of q=0.11 is to enhance the occurrence probability of the low cost. Obviously, such probabilistic cost management purpose is achieved because the cost CDF in this case is with the most favorable low cost section in comparison to those in the other two cases. Undoubtedly, its high cost section will be the worst due to the hedging effect of the solution caused by the used affine generation control. Furthermore, an interesting phenomenon is that the CDF in the case of q=0.99 almost gets no superiority associated with the high cost section when compared with the CDF in the case of q=0.83. Simply, this is because the decrease of the extra expense induced by the overestimation of WPG is fully overwhelmed by the increase of the cost's EV.

VI. Conclusion

In real power systems, the conventional units generally take the burden to balance the uncertainties of WPG and load. Firstly, an affine generation control which drives conventional units to proportionally balance the total power uncertainty (with respect to its EV). So, the quantile of the cost function can be readily obtained with acceptable accuracy by the proposed linearization of the cost. Then, a novel P-OPF model with a quantile corresponding to a probability value has been constructed. Proper selection of the probability value can approach distinct probabilistic cost management purposes. Moreover, the hedging effect of the solution due to the used affine control is also comprehensively discussed and unveiled, e.g. the solution cannot simultaneously benefit the low cost and high cost sections of the cost's CDF. It is also found that the improvements of the extra expense/saving are generally at the expense of the expected cost. Besides, a customized GMM is proposed to approximate the PDF of WPG so that the impacts of its discontinuities are completely extinguished and very satisfactory overall approximation effect is achieved has been proposed. Thus, owing to an analytical PLF method developed based on such proposed approximation, the chance constraints are introduced in the P-OPF model and readily calculated. Example studies of two modified benchmark systems with multiple wind farms have shown accuracy of the developed PLF method and the effectiveness of the proposed P-OPF model to be satisfactory.

Appendix

Data A: Distribution of wind speed is modeled as Weibull with scale parameter of 15m/s and shape parameter of 1.6; The rating of wind turbine is 2MW, and there are 200 wind turbines of the same specifications in each wind farm; The cut-in, cut-off and rated wind speeds of the wind turbine are 4m/s, 22m/s and 12m/s, respectively; and the power curve between cut-in and rated wind speeds is linearly modeled [21].

Data B: Wind speed is normally distributed with expectation of 13m/s and standard deviation of 6m/s; The rating of wind turbine is 2MW and there are 200 wind turbines of the same specifications in each wind farm; The cut-in, cut-off and rated wind speeds of the wind turbine are 4m/s, 27m/s and 15m/s, respectively; and the quadratic model is used to depict the power curve between cut-in and rated wind speeds [25].

References

[1] L. Wang, C. Singh, and A. Kusiak, "Guest editorial: special issue on integration of intermittent renewable energy resources into power grid," *IEEE Syst. J.*, vol. 6, no. 1, pp. 2-3, Mar. 2012.
[2] P. Pinson and G. Kariniotakis, "Conditional prediction intervals of wind power generation,"*IEEE Trans. Power Syst.*,vol. 25, no. 4, pp. 1845-1856, Nov. 2010.
[3] Y. Li, W. Li, W. Yan, J. Yu, and X. Zhao, "Probabilistic optimal power flow considering correlations of wind speeds following different distributions," *IEEE Trans. Power Syst.*,vol. 29, no. 4, pp. 1847-1854, Jul. 2014.
[4] C. S. Saunders, "Point estimate method addressing correlated wind power for probabilistic optimal power flow," *IEEE Trans. Power Syst.*,vol. 29, no. 3, pp. 1045-1054, May 2014.
[5] B. Ren and C. Jiang, "A review on the economic dispatch and risk management considering wind power in the power market," *Renewable Sustainable Energy Rev.*, vol. 13, no. 8, pp. 2169-2174, 2009.
[6] G. Verbic and C. A. Canizares, "Probabilistic optimal power flow in electricity markets based on a two-point estimate method," *IEEE Trans. Power Syst.*,vol. 21, no. 4, pp. 1883-1893, Nov. 2006.
[7] X. Li, Y. Li, and S. Zhang, "Analysis of probabilistic optimal power flow taking account of the variation of load power," *IEEE Trans. Power Syst.*,vol. 23, no. 3, pp. 992-999, Nov. 2008.
[8] M. Madrigal, K. Ponnambalam, and V. H. Quintana, "Probabilistic optimal power flow," in *Proc. IEEECan. Conf. Electrical and Computer Engineering*, Waterloo, ON, Canada, May 1998, pp. 385-388.
[9] A. Schellenberg, W. Rosehart, and J. Aguado, "Cumulant-based probabilistic optimal power flow (P-OPF) with Gaussian and gamma distributions," *IEEE Trans. Power Syst.*,vol. 20, no. 2, pp. 773-781, May 2005.
[10] A. Tamtum, A. Schellenberg, and W. Rosehart, "Enhancements to the cumulant method for probabilistic optimal power flow studies," *IEEE Trans. Power Syst.*,vol. 24, no. 4, pp. 1739-1746, Nov. 2009.
[11] X. Liu and W. Xu, "Economic load dispatch constrained by wind power availability: a here-and-now approach," *IEEE Trans. Sustain. Energy*, vol. 1, no. 1, pp. 2-9, Apr. 2010.
[12] H. Yu and W. D. Rosehart, "An optimal power flow algorithm to achieve robust operation considering load and renewable generation uncertainties," *IEEE Trans. Power Syst.*,vol. 27, no. 4, pp. 1808-1817, Nov. 2012.
[13] R. A. Jabr and B. C. Pal, "Intermittent wind generation in optimal power flow dispatching," *IET Gener. Transm. Distrib.*, vol. 3, no. 1, pp. 66-74, 2009.
[14] J. Hetzer, D. C. Yu, and K. Bhattarai, "An economic dispatch model incorporating wind power," *IEEE Trans. Energy Convers.*,vol. 23, no. 2, pp. 603-611, Jun. 2008.
[15] L. Shi, C. Wang, L. Yao, and Y. Ni, "Optimal power flow solution incorporating wind power," *IEEESyst. J.*, vol. 6, no. 2, pp. 233-241, Jun. 2012.
[16] C.Hamon,M.Perninge, and L.Soder, "The value of using chance-constrained optimal power flows for generation re-dispatch under uncertainty with detailed security constraints"in Power and Energy Engineering Conference (APPEEC), Jul. 12-14, 2013, pp. 1-6.
[17] H. Zhang and P. Li, "Chance constrained programming for optimal power flow under uncertainty," *IEEE Trans. Power Syst.*,vol. 26, no. 4, pp. 2417-2424, Nov. 2011.
[18] M.Kloppel, A.Gabash, A.Geletu, and P. Li,"Chance constrained optimal power flow with non-Gaussian distributed uncertain wind power generation,"in Environment and Electrical Engineering (EEEIC), 12th International Conference, May 5-8, 2013,pp. 265-270.
[19] Y. Cao, Y. Tan, C.Li, andC. Rehtanz,"Chance-constrained optimization-based unbalanced optimal power flow for radial distribution networks,"*IEEE Trans. Power Del.*,vol. 28, no. 3, pp. 1855-1864, Jul.2013.
[20] D. Bienstock, M. Chertkov, and S. Harnett, "Robust modeling of probabilistic uncertainty in smart Grids: data ambiguous chance constrained optimum power flow," in Decision and Control, 52nd IEEE Conference, Dec. 10-13, 2013, pp. 4335-4339.
[21] R. A. Jabr, "Adjustable robust OPF with renewable energy sources," *IEEE Trans. Power Syst.*,vol. 28, no. 4, pp. 4742-4751, Nov. 2013.

[22] H. Zhang and P. Li, “Probabilistic analysis for optimal power flow under uncertainty,”*IET Gener. Transm. Distrib.*, vol. 4, no. 5, pp. 553-561, 2010.
[23] P. Zhang and S. T. Lee, “Probabilistic load flow computation using method of combined cumulants and Gram-Charlier expansion,” *IEEE Trans. Power Syst*.,vol. 19, no. 1, pp. 676-682, Feb. 2004.
[24] S. Blinnikov and R. Moessner, “Expansions for nearly Gaussian distributions,” *Astron. Astrophys. Suppl. Ser*. 130, pp. 193-205, 1998.
[25] J. Usaola, “Probabilistic load flow in systems with wind generation,” *IETGener. Transm. Distrib*., vol. 3, no. 12, pp. 1031-1041, 2009.
[26] M. Fan, V. Vittal, G. T. Heydt, and R. Ayyanar, “Probabilistic power flow studies for transmission systems with photovoltaic generation using cumulants,” *IEEE Trans. Power Syst*.,vol. 27, no. 4, pp. 2251-2261, Nov. 2012.
[27] H. Yu, C. Y. Chung, K. P. Wong, and J. H. Zhang, “A chance constrained transmission network expansion planning method with consideration of load and wind farm uncertainties,” *IEEE Trans. Power Syst*.,vol. 24, no. 3, pp. 1568-1576, Aug. 2009.
[28] S. Q. Bu, W. Du, H. F. Wang, Z. Chen, L. Y. Xiao, and H. F. Li, “Probabilistic analysis of small-signal stability of large-scale power systems as affected by penetration of wind generation,” *IEEE Trans. Power Syst*.,vol. 27, no. 2, pp. 762-770, May 2012.
[29] R. Singh, B. C. Pal, and R. A. Jabr, “Statistical representation of distribution system loads using Gaussian mixture model,” *IEEE Trans. Power Syst*.,vol. 25, no. 1, pp. 29-37, Feb. 2010.
[30] G. Valverde, A. T. Saric, and V. Terzija, “Probabilistic load flow with non-Gaussian correlated random variables using Gaussian mixture models,” *IETGener. Transm. Distrib*., vol. 6, no. 7, pp. 701-709, 2012.
[31] D. Villanueva, J. L. Pazos, and F. Feijoo, “Probabilistic load flow including wind power generation,” *IEEE Trans. Power Syst*.,vol. 26, no. 3, pp. 1659-1667, Aug. 2011.
[32] P.-H. Chen and H.-C. Chang, “Large-scale economic dispatch by genetic algorithm,”*IEEE Trans. Power Syst*.,vol. 10, no. 4, pp. 1919-1926, Nov. 1995.
[33] N. Sinha, R. Chakrabarti, and P. K. Chattopadhyay, “Evolutionary programming techniques for economic load dispatch,” *IEEE Trans.Evol. Comput*., vol. 7, no. 1, pp. 83-94, Feb. 2003.
[34] U. A. Ozturk, M. Mazumdar, and B. A. Norman, “A solution to the stochastic unit commitment problem using chance constrained programming,” *IEEE Trans. Power Syst*.,vol. 19, no. 3, pp. 1589-1598, Aug. 2004.
[35] D. C. Montgomery and G. C. Runger, *Applied Statistics and Probability for Engineers 5th Edition*. John Wiley&Sons, 2010.
[36] D. Pozo and J. Contreras, “A chance-constrained unit commitment with an *n-K* security criterion and significant wind generation,”*IEEE Trans. Power Syst*.,vol. 28, no. 3, pp. 2842-2851, Aug. 2013.
[37] M. Mazadi, W. D. Rosehart, O. Malik, and J. Aguado, “Modified chance-constrained optimization applied to the generation expansion problem,”*IEEE Trans. Power Syst*.,vol. 24, no. 3, pp. 1635-1636, Aug. 2009.
[38] M. Hajian, M. Glavic, W. D. Rosehart, and H. Zareipour, “A chance-constrained optimization approach for control of transmission voltages,”*IEEE Trans. Power Syst*.,vol. 27, no. 3, pp. 1568-1576, Aug. 2012.
[39] W. Van Ackooij, R. Zorgati, R. Henrion, and A. Möller, “Joint chance constrained programming for hydro reservoir management,” Optimization and Engineering, vol. 15, pp. 509-531, 2014.
[40] R. A. Jabr, “Robust self-scheduling under price uncertainty using conditional value-at-risk,” *IEEE Trans. Power Syst*.,vol. 20, no. 4, pp. 1852-1858, Nov. 2005.
[41] Q. Zhang and X. Wang, “Hedge contract characterization and risk constrained electricity procurement,” *IEEE Trans. Power Syst*.,vol. 24, no. 3, pp. 1547-1558, Aug. 2009.
[42] A. Botterud, Z. Zhou, J. Wang, R. J. Bessa, H. Keko, J. Sumaili, and V. Miranda, “wind power trading under uncertainty in LMP markets,”*IEEE Trans. Power Syst*.,vol. 27, no. 2, pp. 894-903, May 2012.
[43] M. Perninge, and L. Soder, “A stochastic control approach to manage operational risk in power systems,”*IEEE Trans. Power Syst*.,vol. 27, no. 2, pp. 1021-1031, May 2012.
[44] Y. Zhang and G. B. Giannakis, “Robust optimal power flow with wind integration using conditional value-at-risk,” in Smart Grid Communications, 2013 IEEE International Conference, Oct. 21-24, 2013, pp. 654-659.
[45] A. Schreiner, G. Balzer, and A. Precht, “Risk analysis of distribution Systems using value at risk methodology,” in Probabilistic Methods Applied to Power Systems, Proceedings of the 10th International Conference, May 25-29, 2008, pp. 1-8.
[46] Y. W. Law, T. Alpcan, and M. Palaniswami, “Security games for risk minimization in automatic generation control,”*IEEE Trans. Power Syst*.,vol. 30, no.1, pp. 223-232, Jan. 2015.
[47] S. Mei, F. He, X. Zhang, S. Wu, and G. Wang, “An improved OPA model and blackout risk assessment,”*IEEE Trans. Power Syst*.,vol. 24, no. 2, pp. 814-823, May 2009.
[48] J. Nocedal and S. J. Wright, *Numerical Optimization*. New York: Springer, 2006.
[49] RTS Task Force of the APM Subcommittee, “IEEE reliability test system,” *IEEE Trans. Power Apparatus Syst*., vol. PAS-98, no. 6, pp. 2047-2054, Nov.-Dec. 1979.
[50] Power System Test Case Archive. [Online]. Available: http://www.ee.washington.edu/research/pstca.

Deping Ke received the B.S degree in Electrical Engineering in 2005 from Huazhong University of Science and Technology, Wuhan, China, and the Ph.D. degree in Electrical Engineering from The Hong Kong Polytechnic University in 2012. Currently, he is a lecturer with the School of Electrical Engineering, Wuhan University, China. His research interests are in power system dynamics and control, and economic operation of power systems.

C. Y. Chung (M’01–SM’07) received the Ph.D. degree in electrical engineering from The Hong Kong Polytechnic University in 1999. He is currently a Professor and the SaskPower Chair in Power Systems Engineering in the Department of Electrical and Computer Engineering at the University of Saskatchewan, Saskatoon, SK, Canada. His research interests include power system stability/control, planning and operation, computational intelligence applications, power markets, and electric vehicle charging. Dr. Chung is an Editor of the IEEE TRANSACTIONS ON SUSTAINABLE ENERGY and an Editorial Board Member of IET GENERATION, TRANSMISSION & DISTRIBUTION. He is also a Member-at-Large (Smart Grid) of IEEE PES Governing Board and the IEEE PES Region 10 North Chapter Representative.

Yuanzhang Sun(M’99-SM’01) received the B.S. degree from Wuhan University of Hydro and Electrical Engineering, Wuhan, China, in 1987, the M.S. degree from the Electric Power Research Institute(EPRI), Beijing, China, in 1982, and the Ph.D. degree in electrical engineering from Tsinghua University, Beijing, in 1988.

Currently, he is a Professor of the School of Electrical Engineering at Wuhan University, and a Chair Professor of the Department of Electrical Engineering and Vice Director of the State Key Lab of Power System Control and Simulation at Tsinghua University. His main research interests are in the areas of power system dynamics and control, wind power, voltage stability and control, and reliability.